

DOI: <https://doi.org/10.24425/amm.2023.142462>RAFIZA ABD RAZAK<sup>1,2\*</sup>, SH. NUR SYAMIMI SY. IZMAN<sup>2</sup>, MOHD MUSTAFA AL BAKRI ABDULLAH<sup>1</sup>,  
ZARINA YAHYA<sup>1,2</sup>, ALIDA ABDULLAH<sup>1</sup>, ROSNITA MOHAMED<sup>1</sup>

## PROPERTIES AND MORPHOLOGY OF FLY ASH BASED ALKALI ACTIVATED MATERIAL (AAM) PASTE UNDER STEAM CURING CONDITION

This paper details the properties, microstructures, and morphologies of the fly ash-based alkali-activated material (AAM), also known as geopolymers, under various steam curing temperatures. The steam curing temperature result in subsequent high strengths relative to average curing temperatures. However, detailed studies involving the use of steam curing for AAM remain scarce. The AAM paste was prepared by mixing fly ash with an alkali activator consisting of sodium silicate ( $\text{Na}_2\text{SiO}_3$ ) and sodium hydroxide ( $\text{NaOH}$ ). The sample was steam cured at 50°C, 60°C, 70°C, and 80°C, and the fresh paste was tested for its setting time. The sample also prepared for compressive strength, density, and water absorption testings. It was observed that the fastest time for the fly ash geopolymer to start hardening was at 80°C at only 10 minutes due to the elevated temperature quickening the hydration of the paste. The compressive strength of the AAM increased with increasing curing time from 3 days to 28 days. The AAM's highest compressive strength was 61 MPa when the sample was steam cured at 50°C for 28 days. The density of AAM was determined to be  $\sim 2122$   $2187 \text{ kg/m}^3$ , while its water absorption was  $\sim 6.72$ - $8.82\%$ . The phase analyses showed the presence of quartz, srebrodolskite, fayalite, and hematite, which indirectly confirms Fe and Ca's role in the hydration of AAM. The morphology of AAM steam-cured at 50°C showed small amounts of unreacted fly ash and a denser matrix, which resulted in high compressive strength.

*Keywords:* Alkali activated material (AAM); geopolymer; fly ash; steam-cured; high-Fe

### 1. Introduction

Steam curing is a process that involves exposing concrete, cement, and mortar to warm steam for hardening. It cures the materials quicker and more uniformly relative to other processes. The hydration and hardening induced by heat and moisture occur at a faster rate due to its more intricate penetration of the materials during exposure, which means that hardened products can be produced quickly using steam curing relative to traditional curing approaches. Steam curing also results in increased strengths, rendering steam-cured materials suitable for use in the construction industry.

Pre-cast and pre-stressed reinforced concrete demonstrate higher strength gains at very early ages [1], which satisfies the need for high mechanical performance material. Thus, steam curing can be as an alternative to solve this issue in which it allows pastes or concrete utilizing admixture to realize faster strength [2], which predominantly affect other properties too [3].

Other than early strength, the hydration process is also of interest to researchers [4,5]. Mengyuan Li et al. (2017) [6] stated that rapid progress of concrete mechanical strength occurs during early ages then gradually increases with increasing age when steam-cured. Therefore, it can be surmised that higher steam curing temperatures increase the hydration rates and increase the overall strength of the resulting products [7].

Geopolymer is a type of inorganic polymer that performs well when steam-cured [8-12]. The term alkali-activated material (AAM) is preferred when its raw material is rich in calcium (Ca), silica (Si), and alumina (Al), then activated in a highly alkaline solution. It is similar to the Ordinary Portland Cement (OPC) in that it forms a solid binder via the hydration process [13]. Despite using the OPC concrete's admixture, AAM is regarded as an alternative concrete suitable for precast and prestressed concrete applications. One major strength of AAM is its removal of OPC usage (only using pozzolanic material as raw materials), and its decrease of greenhouse gas (GHG) discharges [14].

<sup>1</sup> UNIVERSITI MALAYSIA PERLIS, GEOPOLYMER AND GREEN TECHNOLOGY, CENTER OF EXCELLENCE (CEGEOGTECH), KANGAR, MALAYSIA

<sup>2</sup> UNIVERSITI MALAYSIA PERLIS (UNIMAP), FACULTY OF CIVIL ENGINEERING TECHNOLOGY, PERLIS, MALAYSIA

\* Corresponding author: rafizarazak@unimap.edu.my



Geopolymers' excellent properties such as high early strengths, excellent resistance against acid and sulfate attacks, and good performance at high temperatures have been reported in the literature [15].

High early quality is paramount to pre-cast and pre-stressed concrete units due to its requirement for costly structures or stress beds. A common problem faced by the aforementioned concrete is the need to remove its forms as soon as possible and shifting its units to a warehouse. Pre-cast and pre-stressed concrete units are currently prevalent as contractors want to ensure their buildings are completed on time and of high quality. Steam curing quickens early age strength gains; however, steam could influence strength at later ages if its usage is left uncontrolled. Based on previous research, fly ash was reported to possess the best properties when incorporated into geopolymers or AAM concrete. However, research on the performance of fly ash-based AAM under steam curing conditions remains scarce. This paper details the investigation into the physicochemical and microstructural properties of the fly ash-based AAM under various steam curing temperatures.

## 2. Experimental procedure

### 2.1. Raw material

The fly ash is a by-product of pulverized coal-burning sourced from an electric power generating plant. This study's alkali activator is a mixture of sodium silicate ( $\text{Na}_2\text{SiO}_3$ ) and sodium hydroxide (NaOH) solutions. The sodium silicate has a chemical composition of 60.5%  $\text{H}_2\text{O}$ , 30.1% Silica, and 9.4% Sodium Oxide (modulus  $\text{SiO}_2/\text{Na}_2\text{O} = 3.2$ ). The NaOH powder used in this study was 99% pure and had a concentration of 12M.

### 2.2. Mix design and process

The ratio of fly ash/alkali activator was 2.0, while the ratio of  $\text{Na}_2\text{SiO}_3/\text{NaOH}$  used was 2.5 with a NaOH concentration of 12 M. The ratios were kept constant throughout the study. The sodium hydroxide (NaOH) solution was produced by diluting the pellets in distilled water as per the preset concentrations, then cooling at room temperature 24 hours.

The sodium hydroxide (NaOH) and sodium silicate ( $\text{Na}_2\text{SiO}_3$ ) solutions were mixed until homogenous to produce the alkali activator, which was then used to synthesize the fly ash.

The fly ash was mixed with an alkali activator for the concrete mixing process until homogenous to form the AAM paste. The paste was then prepared for Vicat tested to determine its setting and hardening times. The paste was also molded into a cube measuring  $50 \text{ mm} \times 50 \text{ mm} \times 50 \text{ mm}$ , then steam cured at  $50^\circ\text{C}$ ,  $60^\circ\text{C}$ ,  $70^\circ\text{C}$ , and  $80^\circ\text{C}$  for the time required for the paste to set (based on the results obtained from the time setting tested as per ASTM C 191-99. The samples were then exposed to ambient surroundings for 3, 7, and 28 days. The fly ash-based

AAM steam-cured chemical composition at  $50^\circ\text{C}$  was determined using the X-Ray Fluorescence, and the results are shown in TABLE 1.

TABLE 1

The chemical composition of fly ash-based-AAM under steam-cured of  $50^\circ\text{C}$

Compound	$\text{SiO}_2$	$\text{Al}_2\text{O}_3$	$\text{CaO}$	$\text{Fe}_2\text{O}_3$	$\text{MgO}$	$\text{SO}_3$	$\text{K}_2\text{O}$	$\text{TiO}_2$
Composition (%)	35.1	9.46	21.3	25.56	2.3	1.83	1.48	0.95

## 2.3. Testing and analyses

The fly ash-based-AAM's compressive strengths under steam curing were determined experimentally as per the ASTM C109. The samples' densities were determined per the ASTM C1634, while its water absorptions were determined per the ASTM C109. The samples' phase was determined using the X-Ray Diffraction (XRD), while its microstructures were imaged using the Scanning Electron Microscope (SEM).

## 3. Results and discussion

### 3.1. Setting time

Fig. 1 shows the results of the setting times at various steam cured temperatures for the AAM paste. Higher temperatures decrease the time required for the fly ash-based-AAM paste to begin hardening. At  $50^\circ\text{C}$ , it requires 15 minutes (resulted in the highest strength), followed by  $60^\circ\text{C}$ , which requires 13 minutes,  $70^\circ\text{C}$ , requiring 11 minutes, and finally at  $80^\circ\text{C}$ , requiring only 10 minutes. The AAM paste setting time is lower when the steam curing temperature is high(er), which could be due to the expansion induced by the curing temperature hastening the rate of chemical interactions between the fly ash and the alkali activator, thus quickening the hydration process [16,17]. This low setting time is advantageous when using the samples in precast and prestressed concretes, both of which can be demolded faster.

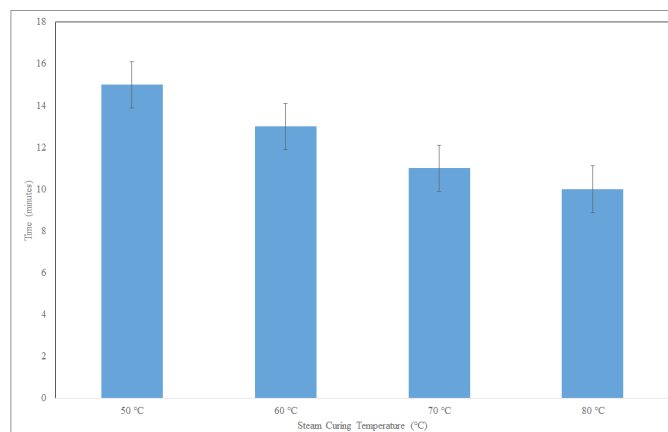


Fig. 1. Setting time of AAM paste under various steam curing condition

### 3.2. Density

The density of AAM paste is  $\sim 2122$ – $2187 \text{ kg/m}^3$ , as per Fig. 2. It can be seen from the bar chart that the highest density is  $2187.84 \text{ kg/m}^3$ , corresponding to a steam curing temperature of  $60^\circ\text{C}$  and curing time of 7 days. The lowest density value is  $2122.32 \text{ kg/m}^3$ , corresponding to a steam curing temperature of  $70^\circ\text{C}$  and curing time of 7 days. The results confirmed a negligible difference between the AAM paste's density at steam curing temperatures of  $50$ – $80^\circ\text{C}$ . The density went up to  $\sim 2187 \text{ kg/m}^3$ . The development of the density can be observed via the increment of curing days, representing the development of the matrix increasing in tandem with aging. The uniformity of the sample during the mixing process could affect the density. The fast reaction between AAM and the alkali activator also influenced the formed matrix's homogeneity, thus affecting the samples' uniformity. However, the density of AAM can be controlled via its ratio to suit a specific application.

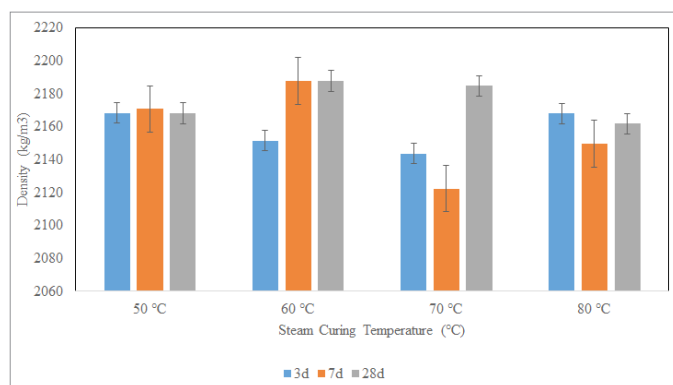


Fig. 2. The density of fly ash-based-AAM paste

### 3.3. Water absorption

Fig. 3 shows the water absorption of the fly ash-based-AAM paste at various steam curing temperatures for 3, 7, and 28 days. The differences between the values are small, within  $\sim 6.72$ – $8.82\%$ . The water absorption confirmed that it is dictated primarily by curing age (up to 28 days in this study), making it suitable for use in concrete. Steam curing is believed to be a suitable curing process as it produces superior surface hardness and better water tightness that prevents moisture from entering

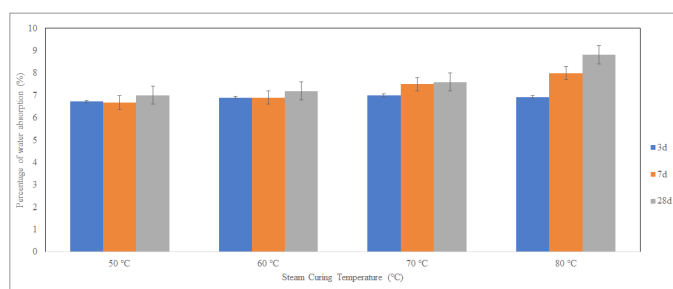


Fig. 3. Graph for water absorption of fly ash-based-AAM under various steam curing temperatures

the sample, which increases the performance and durability of the AAM paste or concrete.

### 3.4. Compressive strength

Fig. 4 shows the compressive strength of the fly ash-based-AAM paste steam cured at  $50$ – $80^\circ\text{C}$  for 3–28 days. It can be seen that the compressive strengths increase in tandem with the increasing curing age of  $\sim 3$ –28 days. The highest compressive strength of  $61 \text{ MPa}$  was obtained from steam curing at  $50^\circ\text{C}$  for 28 days. The sample's strength obtained from steam curing at  $50^\circ\text{C}$  for 28 days ( $30.5 \text{ MPa}$ ) is double that obtained from curing the sample at the same temperature but only for three days. The lowest compressive strength of the AAM paste, at  $25.4 \text{ MPa}$ , was obtained when the sample was steam cured at  $60^\circ\text{C}$  for 3 days. These values confirmed that higher steam curing temperatures do not necessarily result in higher compressive strengths and vice versa. The optimal hydration or geopolymerization rate occurred at the steam curing temperature of  $50^\circ\text{C}$ , resulting in the best compressive strength. Exceeding  $50^\circ\text{C}$  could disrupt the formation of geopolymer matrices as the particles could be disordered when hardening, which decreases the strength of the AAM samples. The lack of moisture is expected to result in inferior quality products due to the paste's unreacted cementitious materials [16,18]. High temperatures could decrease the amount of water required during the hydration process; however, the paste might not realize its best physicomechanical properties [19,20]. It should also be pointed out that too high a temperature would result in the materials not forming well. The negative outcome of steam curing could be exacerbated over time.

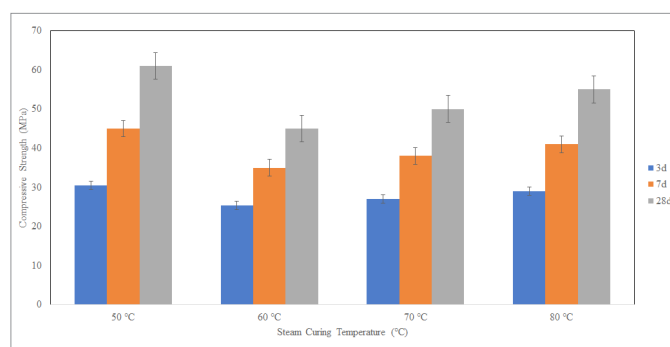


Fig. 4. Compressive strength of fly ash geopolymer at various steam curing temperatures

### 3.5. X-Ray Diffraction

The XRD results ( $2\theta$  of  $10^\circ$ – $50^\circ$ ) of the fly ash-based-AAM paste at various steam curing temperatures are shown in Fig. 5. The five prominent peaks are quartz ( $\text{SiO}_2$ ) at  $26.9^\circ$ , screbrodolskite ( $\text{Ca}_2\text{Fe}_2\text{O}_5$ ) at  $29.7^\circ$ , fayalite ( $\text{Fe}_2\text{SiO}_4$ ) at  $34.0^\circ$ , and hematite ( $\text{Fe}_2\text{O}_3$ ) at  $36.8^\circ$  and  $43.9^\circ$ . Broad humps can be observed at  $28^\circ$ – $37^\circ$  for all conditions. The decrease of the broad hump can be observed at a steam curing temperature of  $80^\circ\text{C}$ ,

which confirms that the formation of the AAM matrix was complete, agreeing with the compressive strength of the samples increasing at 80°C relative to 60°C and 70°C. The presence of srebrodolskite, fayalite, and hematite suggests that Ca and Fe contribute to the AAM system's strength. Kaze et al. (2018) [21] and Warid et al. [22] claimed that the formation of fayalite could occur via a chemical reaction of hydrated ferric oxyhydroxide with silica, which is in line with the chemical composition of AAM paste showing high percentages of Fe and Ca.

### 3.6. Morphology analysis

The morphology of the AAM samples at various steam curing temperatures at 3 days of aging was imaged using an SEM at a magnification of 2000×, and the results are shown in Fig. 6. It can be seen that the hardening and hydration processes of the AAM, or geopolymerization, remained incomplete. The images showed that the fly ash dissolution in the alkali activator remained incomplete, confirmed via the presence of pores and voids in the AAM matrix. However, Fig. 6(a) shows the formation of the AAM matrix resulting in excellent strength, which gave the fly ash-based-AAM sample steam cured at 50°C the best strength. Incomplete geopolymerization via incomplete dissolution of fly ash in the alkali activator solution was evident in the steam cured samples at 60°C and 70°C, resulting in lower strengths for both. Some microcracks were present in the steam

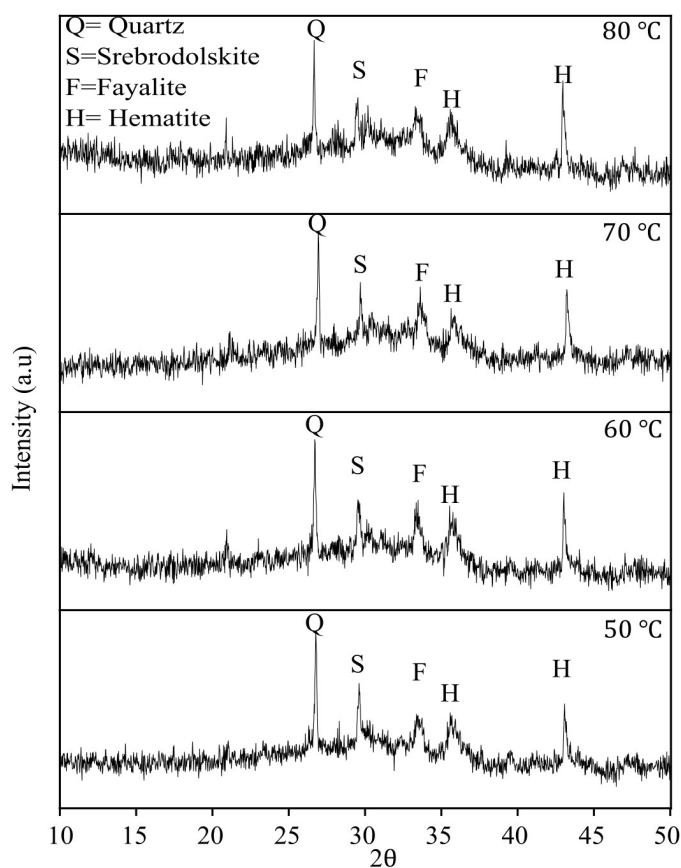


Fig. 5. XRD patterns of fly ash-based-AAM under various steam curing temperatures

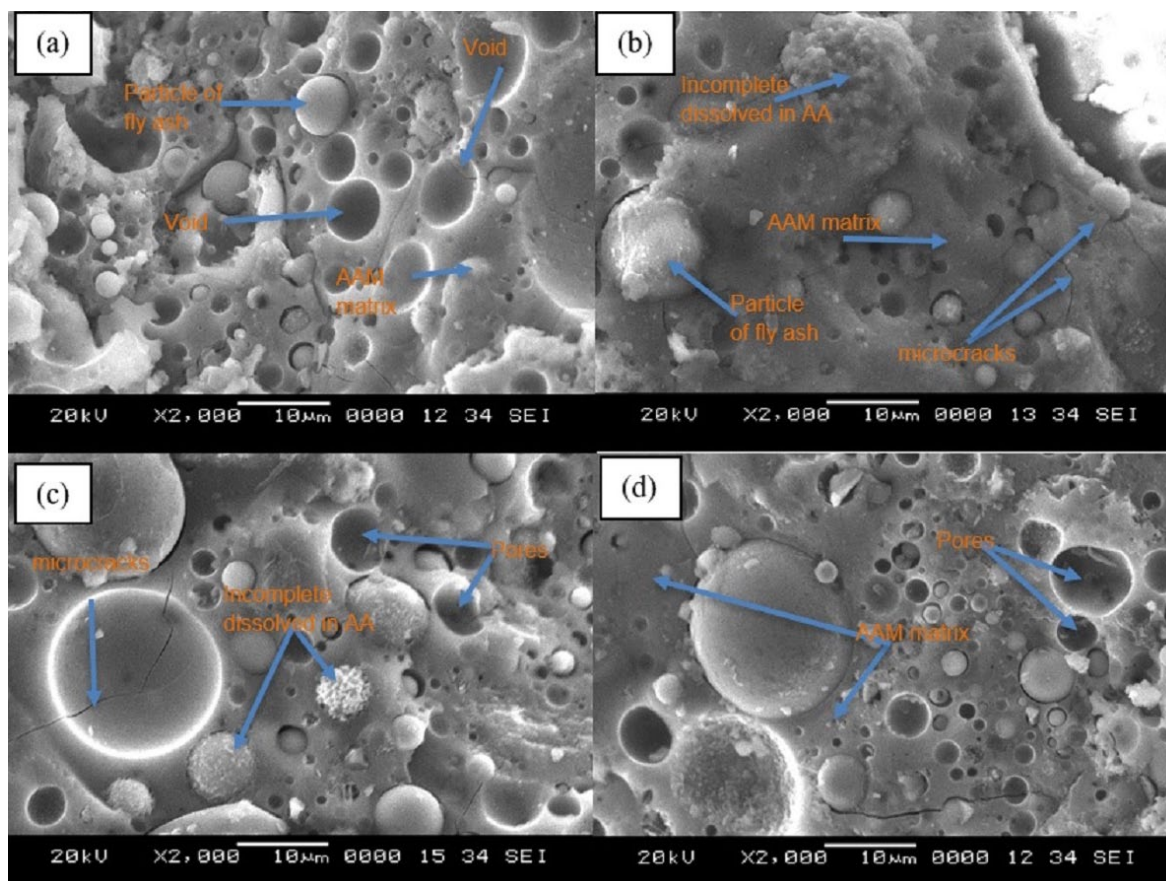


Fig. 6. SEM images of fly ash based AAM at various steam curing temperature; (a) 50°C; (b) 60°C; (c) 70°C; and (d) 80°C



cured 60°C, 70°C and 80°C samples due to the high steam temperature the heat produced during the geopolymerization process, which led to the non-uniform water evaporation during curing [23,24], the occurrence of which decreases the strength of the AAM paste.

#### 4. Conclusion

The steam cured fly ash-based-AAM performance is excellent, possessing a high strength of 30.5 MPa when steam cured for 3 days and 61 MPa when steam cured at 50°C for 28 days. The fastest setting time was reported when the AAM paste was steam cured at 80°C, only requiring 10 minutes to set. The concrete's density was ~2122-2187 kg/m<sup>3</sup>, which is regarded as the average weight for concrete. The water absorption was ~6.72-8.82%, which is acceptable. The phase analyses showed quartz, screbrodolskite, fayalite, and hematite, confirming Fe and Ca's role in the hydration process of the AAM. The morphology of the AAM paste at 50°C steam-cured had lower amounts of unreacted fly ash with an alkali activator and denser matrix, which resulted in high compressive strength. Therefore, it can be concluded that 50°C is the optimum steam curing temperature for fly ash-based-AAM as it results in the best strength, setting time, density, and water absorption for precast or prestressed concretes that require a quick demolding process that can withstand high performance. Its quick hardening can quicken the construction of buildings, which increases efficiency. This study's findings are also a viable alternative for decreasing carbon dioxide (CO<sub>2</sub>), a greenhouse gas that is harmful to the environment.

#### Acknowledgement

The author is grateful and acknowledges the support from the Fundamental Research Grant Scheme (FRGS) 2019 under the grant number 9003-00747 (FRGS/1/2019/TK06/UNIMAP/02/1) from the Ministry of Higher Education Malaysia. The author also would like to acknowledge Geopolymer & Green Technology, Center of Excellence, Universiti Malaysia Perlis (UniMAP) for providing equipment and laboratory in this project. The author is also grateful to the Faculty of Civil Engineering Technology staff for the cooperation given and assistance in the research.

#### REFERENCES

- [1] A. Gonzalez-Corominas, M. Etxeberria, C.S. Poon, *Cement and Concrete Composites* **71**, 77-84 (2016).
- [2] P. Shen, L. Lu, W. Chen, F. Wang, S. Hu, *Construction and Building Materials* **152**, 357-366 (2017).
- [3] S.C. Kou, C.S. Poon, D. Chan, *International RILEM Conference on the Use of Recycled Materials in Buildings and Structures, Barcelona* **1**, 590-599 (2004).
- [4] P.H. Klieger, *ACI Journal, Proceeding* **4** (12), 1063-1081 (1958).
- [5] P. Klieger, *Some Aspects of Durability and Volume Change of Concrete for Prestressing, Research Department Bulletin RX118, Portland Cement Association, http://www.portcement.org/pdf\_files/RX118.pdf, 1960, 15 pages.*
- [6] L. Mengyuan, W. Qiang, Y. Jun, *Advances in Materials Science and Engineering*, 2017 (Article ID 9863219), 11 (2017)
- [7] J. Shubham, V. Deepak, B. Suraj, A. Jayesh, K. Rajesh, *International Journal of Architectural Design and Management* **3** (2) (2020).
- [8] N.F. Shahedan, M.M.A.B. Abdullah, N. Mahmed, A. Kusbi-antoro, S. Tammam-Williams, L.Y. Li, I.H. Aziz, P. Vizureanu, J.J. Wysocki, K. Błoch, M. Nabiałek, *Materials* **14**, 809 (2021).
- [9] O.H. Li, L. Yun-Ming, H. Cheng-Yong, R. Bayuaji, M.M.A.B. Abdullah, F.K. Loong, T.A. Jin, N.H. Teng, M. Nabiałek, B. Jeż, N.Y. Sing, *Magnetochemistry* **7** (1), 9 (2021).
- [10] N.H. Jamil, M.M.A.B. Abdullah, F. Che Pa, M. Hasmaliza, W.M.A. Ibrahim, I.H.A. Aziz, B. Jeż, M. Nabiałek, *Magnetochemistry* **7**, 32 (2021).
- [11] R. Ahmad, M.M.A.B. Abdullah, W.M.W. Ibrahim, K. Hussin, F.H. Ahmad Zaidi, J. Chairapra, J.J. Wysocki, K. Błoch, M. Nabiałek, *Materials* **14**, 1077 (2021).
- [12] M.A. Faris, M.M.A.B. Abdullah, R. Muniandy, M.F. Abu Hashim, K. Błoch, B. Jeż, S. Garus, P. Palutkiewicz, N.A. Mohd Mortar, M.F. Ghazali, *Materials* **14**, 1310 (2021).
- [13] W.W.A. Zailani, M.M.A.B. Abdullah, M.F. Arshad, R.A. Razak, M.F.M. Tahir, R.R.M.A. Zainol, M. Nabiałek, A.V. Sandu, J.J. Wysocki, K. Błoch, *Materials* **14**, 56 (2021).
- [14] G. Roviello, C. Menna, O. Tarallo, L. Ricciotti, F. Messina, C. Ferone, R. Cioffi, *Composites Part B: Engineering* **128**, 225-237 (2017).
- [15] Y. Hefni, Y.A. Zaher, M.A. Wahab, *Construction and Building Materials* **172**, 728-734 (2018).
- [16] S. Ismail, W.H. Kwan, M. Ramli, *Construction and Building Materials* **155**, 296-306 (2017).
- [17] M. Rosnita, A.R. Rafiza, A.A.M. Mustafa, S. Raa Khimi, C. Jitrin, *Journal of Non-Crystalline Solids* **553**, 120519 (2021).
- [18] D.D. Burduhos Nergis, P. Vizureanu, O. Corbu, *Revista de Chimie* **70** (4), 1262-1267 (2019).
- [19] S. Türkel, V. Alabas, *Cement and Concrete Research* **35** (2), 405-411 (2005).
- [20] X. Zhuang, Y.C. Liang, K. Sridhar, Z. Chun, H. Tong, *Journal of Cleaner Production* **125**, 253-26 (2016).
- [21] R.C. Kaze, A.L.M.B. Moungam, M. Cannio, R. Rosa, E. Kam-seu U.C. Melo, C. Leonelli, *Journal of Cleaner Production* **199**, 849-859 (2018).
- [22] A.Z. Warid Wazien, B. Aissa, A.M.M. Mustafa, A.R. Rafiza, Y. Sorachon, M.S. Mohd Arif Anuar, M.A.Z. Mohd Remy Rozaini, H. Fansuri, *Applied Sciences* **10** (3321) (2020).
- [23] S. Alehyen, M.E.L. Achouri, M. Taibi, *Journal of Materials and Environmental Sciences* **8** (5), 1783-1796 (2017).
- [24] D.D. Burduhos Nergis, M.M.A.B. Abdullah, A.V. Sandu, P. Vizureanu, *Materials* **13** (2), 343 (2020).